26

Harmonic Generation in Nanoscale Ferroelectric Films

Jeffrey F. Webb
Swinburne University of Technology, Sarawak Campus
Malaysia

1. Introduction

The presence of surfaces or interfaces causes the behavior of ferroelectric materials to differ from that of the bulk, in a way analogous to that for magnetic and superconducting materials(Tilley, 1993; 1996). Here we will be concerned with a theoretical model that takes into account the influence of surfaces on a ferroelectric film. There is also experimental evidence that indicates that size effects in ferroelectrics are observable (Gerbaux & Hadni, 1989; Gerbaux et al., 1989; Höchli & Rohrer, 1982; Kulkarni et al., 1988; Marquardt & Gleiter, 1982; Mishina et al., 2003; Scott & Araujo, 1989) ;more recently, the strong influence of boundaries on ferroelectric behaviour has been demonstrated (Li et al., 1996; 1997).Due to the advent of ferroelectric random access memories (Scott, 1998) size effects in ferroelectric thin films are of increasing importance.

This chapter shows how the Landau-Devonshire theory of ferroelectrics can be applied to thin films and how the dynamic response to incident electromagnetic radiation can be calculated. One aim is to show how harmonic generation components that occur because of the nonlinear response of the ferroelectric can found and in particular how they are reflected from the film. This is done because it relates to reflection measurements that could be carried out on the film to investigate the theoretical proposals experimentally. Since ferroelectrics are responsive in the terahertz region, terahertz wave measurements, especially in the far infrared region would be the most relevant. Another aim is to present a general theory that serves as a foundation for other calculations involving ferroelectric films.

To begin with, the Landau-Devonshire theory for calculating the static polarization is developed starting with a bulk ferroelectric and progressing from a semi-infinite film to one of finite thickness. It is then shown how dynamical equations can be incorporated together with a Maxwell wave equation in order to calculate the dynamic response. This in general is a nonlinear problem and using a standard perturbation expansion technique it is shown how the harmonic components can be isolated and calculated. Finally a specific example of second harmonic generation for a ferroelectric film on a metal substrate is given in which the reflection coefficient is calculated exactly under simplified boundary conditions.

2. Landau-Devonshire theory

The starting point of the Landau-Devonshire theory is the Gibbs free energy expressed as a series expansion in powers of components of the polarization vector **P**. The equilibrium

polarization is found from the minimum of the free energy function; the temperature dependence is such that below the Curie temperature the minimum corresponds to a non-zero polarization but above this temperature it is zero, thus representing one of the basic properties of a ferroelectric. Also the property that the spontaneous polarization can be reversed by the application of an external electric field is manifest in the theory by more than one minimum in the free energy so that the polarization can be switched between different possible equilibrium polarizations. We will need a free energy expression for a ferroelectric film. Here we first develop the ideas for a bulk ferroelectric and a semi-infinite ferroelectric as this is an instructive way to lead up to the thin film case.

2.1 Bulk ferroelectrics

For a bulk ferroelectric a Gibbs free energy of the following form is often used (Lines & Glass, 1977)

$$F = \frac{1}{2}AP^2 + \frac{1}{4}BP^4 + \frac{1}{6}CP^6, \tag{1}$$

where

$$A = a(T - T_{C0}) \tag{2}$$

and

$$P^2 = P_x^2 + P_y^2 + P_z^2. \tag{3}$$

The equilibrium polarization for the bulk ferroelectric is given by the minimum of the free energy, found by solving

$$\frac{\partial F}{\partial P} = 0 \rightarrow AP_B + BP_B^3 + CP_B^5 = 0. \tag{4}$$

For first order transitions, which are discontinuous, $B < 0$ and $C > 0$. But for second order transitions, where the magnitude of the polarization changes continuously from P_B to zero as the temperature is raised through T_{C0}, the term in P^6 can be dropped ($C = 0$) and $B > 0$. a is always a positive constant. The theory is phenomenological so that the parameters described take values that can be found from experiment, or which, in some cases, can be calculated using first-principles methods based on microscopic models of ferroelectrics (Iniguez et al., 2001).

Figure 1 illustrates the behaviour for the second-order case $C = 0$; for $T > T_{C0}$ the minimum of F is at $P = 0$, corresponding to no spontaneous polarization above T_{C0}, the paraelectric phase; and for $T < T_{C0}$ minima occur at $P = \pm P_B$, where

$$P_B = \frac{|A|}{B}. \tag{5}$$

This represents the switchable spontaneous polarization that occurs in the ferroelectric phase.

The free energy in Landau theory is invariant under the symmetry transformations of the symmetry group of the paraelectric phase. The expression in Equation (1) is therefore, in general, only an approximation to the actual free energy. For example, for a cubic ferroelectric such as barium titanate, the paraelectric phase has cubic symmetry and the terms $P_x^4 + P_y^4 + P_z^4$ and $P_x^2P_y^2 + P_y^2P_z^2 + P_z^2P_x^2$ are separately invariant and would need to be included in the free energy. However, as brought out by Strukov & Lenanyuk (1998), for the simplest transition of

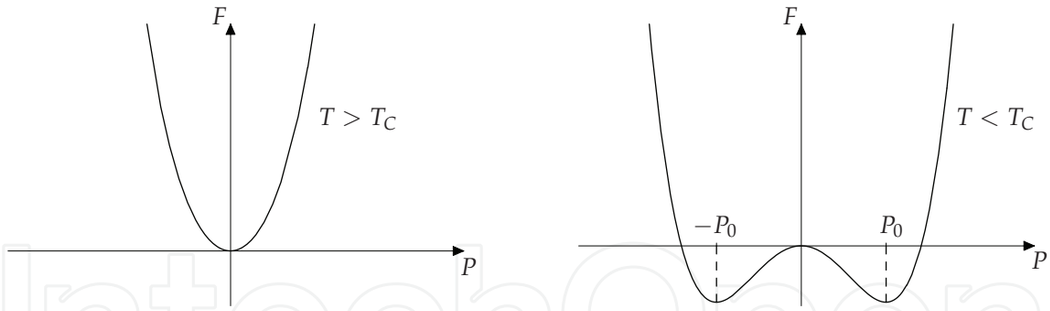

Fig. 1. Landau Free energy above and below T_{C0}.

a perovskite ferroelectric from its cubic paraelectric phase to a tetragonal ferroelectric phase Equation (1) has appropriate symmetry.

2.2 A semi-infinite film

We take the film surface to be in the xy plane of a Cartesian coordinate system, and assume that the spontaneous polarization is in-plane so that depolarization effects (Tilley, 1996) do not need to be taken into account. The spontaneous polarization due to the influence of the surface, unlike in the bulk, may not be constant when the surface is approached. Hence we now have $\mathbf{P} = \mathbf{P}(z)$, and this implies that a term in $|dP/dz|^2$ is present in the free energy expansion together with a surface term (Chandra & Littlewood, 2007; Cottam et al., 1984), and the free energy becomes

$$F = \iint dxdy \int_0^\infty dz \left[\frac{1}{2}AP^2 + \frac{1}{4}BP^4 + \frac{1}{6}CP^6 + \frac{1}{2}D\left(\frac{dP}{dz}\right)^2 \right] + \frac{1}{2}D \iint dx\, dy\, P^2(0)\delta^{-1}, \quad (6)$$

so that the free energy per unit area where S is the surface area of the film is

$$\frac{F}{S} = \int_0^\infty dz \left[\frac{1}{2}AP^2 + \frac{1}{4}BP^4 + \frac{1}{6}CP^6 + \frac{1}{2}D\left(\frac{dP}{dz}\right)^2 \right] + \frac{1}{2}DP^2(0)\delta^{-1}. \quad (7)$$

The surface term includes a length δ which will appear in a boundary condition required when the free energy is minimized to find the equilibrium polarization. In fact, finding the minimum, due to the integral over the free energy expansion, is now the problem of minimizing a functional. The well know Euler-Lagrange technique can be used which results in the following differential equation

$$D\frac{d^2P}{dz^2} - AP - BP^3 - CP^5, \quad (8)$$

with boundary condition

$$\frac{dP}{dz} - \frac{1}{\delta}P = 0, \quad \text{at } z = 0. \quad (9)$$

The solution of the Euler-Lagrange equation with this boundary condition gives the equilibrium polarization $P_0(z)$. It can be seen from Equation (9) that δ is an extrapolation length and that for $\delta < 0$ the polarization increases at the surface and for $\delta > 0$ it decreases at the surface, as is illustrated in Figure 2.

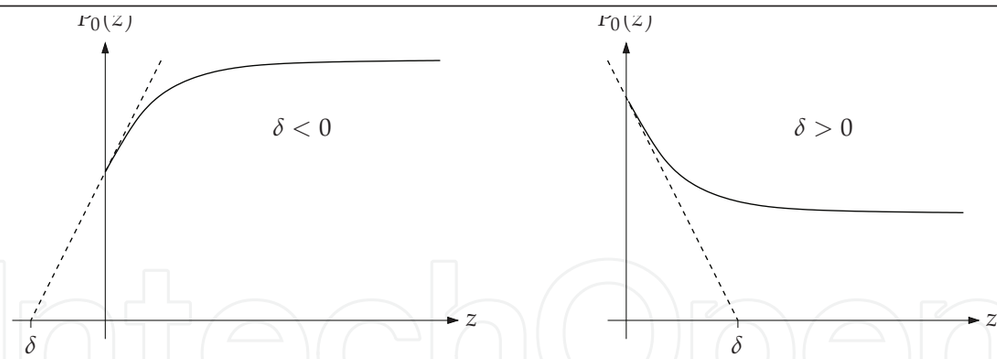

Fig. 2. Extrapolation length δ. For $\delta < 0$ the polarization increases at the surface and for $\delta > 0$ it decreases at the surface. The dotted lines have slopes given by $[dP_0/dz]_{z=0}$.

For first order transitions with $C \neq 0$ the solution to Equation (9) must be obtained numerically (Gerbaux & Hadni, 1990). However for second order transitions ($C = 0$) an analytical solution can be found as will now be outlined. The equation to solve in this case, subject to Equation (9), is

$$D\frac{d^2P}{dz^2} - AP - BP^3. \tag{10}$$

The first integral is

$$\frac{1}{2}D\left(\frac{dP}{dz}\right)^2 - \frac{1}{2}AP^2 - \frac{1}{4}BP^4 = G, \tag{11}$$

and since as $z \to \infty$, P tends to its bulk value P_B while $dP/dz \to 0$,

$$G = (1/2)AP_{\text{bulk}}^2 - (1/4)BP_{\text{bulk}}^4. \tag{12}$$

For $T < T_{C0}$, we take $P_{\text{bulk}} = P_B$, where P_B is given by Equation (5) and $G = A^2/4B$. Following Cottam et al. (1984), integration of Equation (11) then gives

$$P_0(z) = P_B \coth[(z + z_0)/\sqrt{2}\xi], \quad \text{for } \delta < 0, \tag{13}$$

$$P_0(z) = P_B \tanh[(z + z_0)/\sqrt{2}\xi], \quad \text{for } \delta > 0, \tag{14}$$

where ξ is a coherence length given by

$$\xi^2 = \frac{D}{|A|}. \tag{15}$$

Application of the boundary condition, Equation (9), gives

$$z_0 = (\xi\sqrt{2}\sinh^{-1}(\sqrt{2}|\delta|/\xi). \tag{16}$$

Plots of Equations (13) and (14) are given by Cottam et al. (1984).
For the $\delta < 0$ case in which the polarization increases at the surface it can be shown (Cottam et al., 1984; Tilley, 1996), as would be expected, that the phase transition at the surface occurs at a higher temperature than the bulk; there is a surface state in the temperature range $T_{C0} < T < T_C$. For $\delta > 0$, the polarization turns down at the surface and it is expected that the critical temperature T_C at which the film ceases to become ferroelectric is lower than T_{C0}, as has been brought out by Tilley (1996) and Cottam et al. (1984).

2.3 A finite thickness film

Next a finite film is considered. The thickness can be on the nanoscale, where it is expected that the size effects would be more pronounced. The theory is also suitable for thicker films; then it is more likely that in the film the polarization will reach its bulk value.

The free energy per unit area of a film normal to the z axis of thickness L, and with in-plane polarization again assumed, can be expressed as

$$\frac{F}{S} = \int_{-L}^{0} dz \left[\frac{1}{2}AP^2 + \frac{1}{4}BP^4 + \frac{1}{6}CP^6 + \frac{1}{2}D\left(\frac{dP}{dz}\right)^2 \right] + \frac{1}{2}D\left[P^2(-L)\delta_1^{-1} + P^2(0)\delta_2^{-1}\right], \quad (17)$$

which is an extension of the free energy expression in Equation (7) to include the extra surface. Two different extrapolation lengths are introduced since the interfaces at $z = -L$ and $z = 0$ might be different—in the example below in Section 5.2 one interface is air-ferroelectric, the other ferroelectric-metal. The Euler-Lagrange equation for finding the equilibrium polarization is still given by Equation (8) and the boundary conditions are

$$\frac{dP}{dz} - \frac{1}{\delta_1}P = 0, \quad \text{at } z = -L, \quad (18)$$

$$\frac{dP}{dz} + \frac{1}{\delta_2}P = 0, \quad \text{at } z = 0. \quad (19)$$

With the boundary conditions written in this way it follows that if $\delta_1, \delta_2 < 0$ the polarization turns up at the surfaces and for $\delta_1, \delta_2 > 0$, it turns down. When the signs of δ_1 and δ_2 differ, at one surface the polarization will turn up; at the other it will turn down.

Solution of the Euler-Lagrange equation subject to Equations (18) and (19) has to be done numerically(Gerbaux & Hadni, 1990; Tan et al., 2000) for first order transitions. Second order transitions where $C = 0$, as for the semi-infinite case, can be found analytically, this time in terms of elliptic functions (Chew et al., 2001; Tilley & Zeks, 1984; Webb, 2006). Again the first integral is given by Equation (11). But now the second integral is carried out from one boundary to the point at which $(dP/dz) = 0$, and then on to the next boundary, and, as will be shown below, G is no longer given by Equation (12) . The elliptic function solutions that result are different according to the signs of the extrapolation lengths. There are four permutations of the signs and we propose that the critical temperature, based on the previous results for the semi-infinite film, will obey the following:

$$\delta_1, \delta_2 > 0 \Rightarrow T_C < T_{C0} \quad (P \text{ increases at both surfaces}), \quad (20)$$

$$\delta_1, \delta_2 < 0 \Rightarrow T_C < T_{C0} \quad (P \text{ decreases at both surfaces}), \quad (21)$$

$$\delta_1 > 0, \delta_2 < 0, |\delta_2| \lesseqgtr |\delta_1| \Rightarrow T_C \lesseqgtr T_{C0} \quad (P \text{ decreases at } z = -L, \text{ increases at } z = 0\ ), \quad (22)$$

$$\delta_1 < 0, \delta_2 > 0, |\delta_1| \lesseqgtr |\delta_2| \Rightarrow T_C \lesseqgtr T_{C0} \quad (P \text{ increases at } z = -L, \text{ decreases at } z = 0\ ). \quad (23)$$

There will be surface states, each similar to that described for the semi-infinite film, for any surfaces for which P increases provided that $T_C > T_{C0}$.

The solutions for the two cases $\delta_1 = \delta_2 = \delta < 0$ and $\delta_1 = \delta_2 = \delta > 0$ will be given first because they contain all of the essential functions; dealing with the other cases will be discussed after that. Some example plots of the solutions can be found in Tilley & Zeks (1984) and Tilley (1996).

2.3.1 Solution for $\delta_1 = \delta_2 = \delta > 0$

Based on the work of Chew et al. (2001), after correcting some errors made in that work, the solution to Equation (10) with boundary conditions (19) and (20) for the coordinate system implied by Equation (17) is

$$P_0(z) = P_1 \,\mathrm{sn}\left[K(\lambda) - \frac{z + L_2}{\zeta}, \lambda\right], \tag{24}$$

where $0 < L_2 < L$[1] and the position in the film at which $dP/dz = 0$ is given by $z = -L_2$ (for a fixed L, the value of L_2 uniquely defined by the boundary conditions); λ is the modulus of the Jacobian elliptic function sn and $K(\lambda)$ is the complete elliptic integral of the first kind (Abramowitz & Stegun, 1972). Also,

$$P_1^2 = -\frac{A}{B} - \sqrt{\frac{A^2}{B^2} - \frac{4G}{B}}, \tag{25}$$

$$P_2^2 = -\frac{A}{B} + \sqrt{\frac{A^2}{B^2} - \frac{4G}{B}}, \tag{26}$$

$$\lambda = \frac{P_1}{P_2}, \quad \text{and} \quad \zeta = \frac{1}{P_2}\sqrt{\frac{2D}{B}}. \tag{27}$$

Although this is an analytic solution, the constant of integration G is found by substituting it into the boundary conditions; this leads to a transcendental equation which must be solved numerically for G.

2.3.2 Solution for $\delta_1 = \delta_2 = \delta < 0$

The equations in this section are also based on the work of Chew et al. (2001), with some errors corrected.

In this case there is a surface state, discussed above when $T_{C0} \leqslant T \leqslant T_C$ and for $T < T_{C0}$ the whole of the film is in a ferroelectric state. In each of these temperature regions the solution to Equation (10) is different.

For the surface state,

$$P_0(z) = \frac{P_2}{\mathrm{cn}\left[\dfrac{z + L_2}{\zeta_1}, \lambda_1\right]}, \quad T_{C0} \leqslant T \leqslant T_C, \tag{28}$$

where

$$\lambda_1 = \left[1 - \left(\frac{P_2}{P_1}\right)^2\right]^{-1}, \quad \zeta_1 = \frac{\lambda}{Q}\sqrt{\frac{2D}{B}}, \quad \text{and} \quad Q^2 = -P_1^2, \tag{29}$$

with P_1, P_2 and L_2 as defined above. G (implicit in P_1 and P_2) has to be recalculated for the solution in Equation (28) and again this leads to a transcendental equation that must be solved numerically.

[1] The reason for the notation L_2, rather than say L_1 is a matter of convenience in the description that follows of how to apply the boundary conditions to find the integration constant G that appear via Equations (25) and (26).

When the whole film is in a ferroelectric state

$$P_0(z) = \frac{P_2}{\mathrm{sn}\left[K(\lambda) - \dfrac{z + L_2}{\zeta}, \lambda\right]}, \quad T < T_C, \tag{30}$$

where K, λ and ζ are as defined above, and G is found by substituting this solution into the boundary conditions and solving the resulting transcendental equation numerically.

2.3.3 Dealing with the more general case $\delta_1 \neq \delta_2$

One or more of the above forms of the solutions is sufficient for this more general case. The main issue is satisfying the boundary conditions. To illustrate the procedure consider the case $\delta_1, \delta_2 > 0$. The polarization will turn down at both surfaces and it will reach a maximum value somewhere on the interval $-L < z < 0$ at the point $z = -L_2$; for $\delta_1 \neq \delta_2$ this maximum will not occur when $L_2 = L/2$ (it would for the δ case considered in Section 2.3.2).

The main task is to find the value of G that satisfies the boundary conditions for a given value of film thickness L. For this it is convenient to make the transformation $z \to z - L_2$. The maximum of P_0 will then be at $z = 0$ and the film will occupy the region $-L_1 \leqslant L \leqslant L_2$, where $L_1 + L_2 = L$. Now the polarization is given by

$$P_0(z) = P_1 \,\mathrm{sn}\left[K(\lambda) - \frac{z}{\zeta}, \lambda\right]. \tag{31}$$

Transforming the boundary conditions, Equations (18) and (19), to this frame and applying them to Equation (31) to the case under consideration ($\delta_1, \delta_2 > 0$) leads to

$$\frac{\delta_1}{\zeta(G)} \,\mathrm{cn}\left[K(\lambda(G)) + \frac{L_1}{\zeta(G)}, \lambda\right] \mathrm{dn}\left[K(\lambda(G)) + \frac{L_1}{\zeta(G)}, \lambda\right] = -\,\mathrm{sn}\left[K(\lambda(G)) + \frac{L_1}{\zeta(G)}, \lambda\right] \quad \text{(bc1)}$$

and

$$\frac{\delta_2}{\zeta(G)} \,\mathrm{cn}\left[K(\lambda(G)) - \frac{L_2}{\zeta(G)}, \lambda\right] \mathrm{dn}\left[K(\lambda(G)) - \frac{L_2}{\zeta(G)}, \lambda\right] = \mathrm{sn}\left[K(\lambda(G)) - \frac{L_2}{\zeta(G)}, \lambda\right]. \quad \text{(bc2)}$$

Here the G dependence of some of the parameters has been indicated explicitly since G is the unknown that must be found from these boundary equations. It is clear that in term of finding G the equations are transcendental and must be solved numerically. A two-stage approach that has been successfully used by Webb (2006) will now be described (in that work the results were used but the method was not explained).

The idea is to calculate G numerically from one of the boundary equations and then make sure that the film thickness is correctly determined from a numerical calculation using the remaining equation. For example, if we start with (bc1), G can be determined by any suitable numerical method; however the calculation will depend not only on the value of δ_1 but also on L_1 such that $G = G(\delta_1, L_1)$. To find the value of L_1 for a given L that is consistent with $L = L_1 + L_2$, (bc2) is invoked: here we require $G = G(\delta_2, L_2) = G(\delta_2, L - L_1) = G(\delta_1, L_1)$, and the value of L_1 to be used in $G(\delta_1, L_1)$ is that which satisfies (bc2). In invoking (bc2) the calculation—which is also numerical of course—will involve replacing L_2 by $L - L_1 = L - L_1[\delta_2, G(\delta_1, L_1)]$. The numerical procedure is two-step in the sense that the (bc1) numerical calculation to find $G(\delta_1, L_1)$ is used in the numerical procedure for calculating L_1 from (bc2)

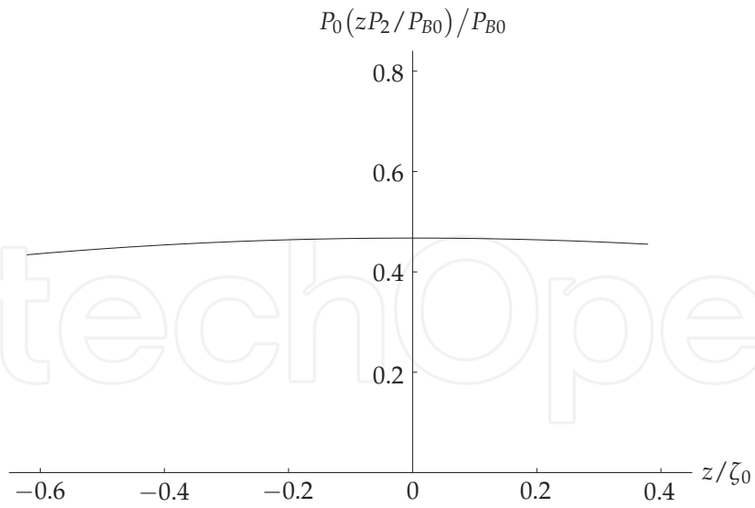

Fig. 3. Polarization versus distance for a film of thickness L according to Equation (31) with boundary conditions (bc1) and (bc2). The following dimensionless variables and parameter values have been used: $P_{B0} = (aT_{C0}/B)^{1/2}$, $\zeta_0 = [2D/(aT_C)]^{1/2}$, $\Delta T' = (T - T_{C0})/T_{C0} = -0.4$, $L' = L/\zeta_0 = 1$, $\delta_1' = 4L'$, $\delta_2' = 7L'$, $G' = 4GB/(a/T_{C0})^2 = 0.127$, $L_1' = L_1/\zeta_0 = 0.621$, $L_1' = L_2/\zeta_0 = 0.379$.

(in which L_2 is written as $L - L_1$). In this way the required L_1 is calculated from (bc2) and L_2 is calculated from $L_2 = L - L_2$. Hence G, L_1 and L_2 have been determined for given values of δ_1, δ_2 and L.

It is worth pointing out that once G has been determined in this way it can be used in the $P_0(z)$ in Equation (24) since the inverse transformation $z \to z + L_2$ back to the coordinate system in which this $P(z)$ is expressed does not imply any change in G.

Figure 3 shows an example plot of $P_0(z)$ for the case just considered using values and dimensionless variables defined in the figure caption.

A similar procedure can be used for other sign permutations of δ_1 and δ_2 provided that the appropriate solution forms are chosen according to the following:

1. $\delta_1, \delta_2 < 0$: use the transformed ($z \to z - L_2$) version of Equation (28) for $T_{C0} \leqslant T \leqslant T_C$, or the transformed version of Equation (30) for $T < T_C$.
2. $\delta_1 > 0, \delta_2 < 0$: for $-L_1 \leqslant L < 0$ use Equation (31); for $0 \leqslant L \leqslant L_2$ follow 1.
3. $\delta_1 < 0, \delta_2 > 0$: for $-L_1 \leqslant L < 0$ follow 1; for $0 \leqslant L \leqslant L_2$ use Equation (31).

3. Dynamical response

In this section the response of a ferroelectric film of finite thickness to an externally applied electric field **E** is considered. Since we are interested in time varying fields from an incident electromagnetic wave it is necessary to introduce equations of motion. It is the electric part of the wave that interacts with the ferroelectric primarily since the magnetic permeability is usually close to its free space value, so that in the film $\mu = \mu_0$ and we can consider the electric field vector **E** independently.

An applied electric field is accounted for in the free energy by adding a term $-\mathbf{P}\cdot\mathbf{E}$ to the expansion in the integrand of the free energy density in Equation (17) yielding

$$\frac{F_E}{S}=\int_{-L}^{0}dz\left[\frac{1}{2}AP^2+\frac{1}{4}BP^4+\frac{1}{6}CP^6+\frac{1}{2}D\left(\frac{dP}{dz}\right)^2-\mathbf{P}\cdot\mathbf{E}\right]+\frac{1}{2}D\Big[P^2(-L)\delta_1^{-1}+P^2(0)\delta_2^{-1}\Big]. \tag{32}$$

In order to find the dynamical response of the film to incident electromagnetic radiation Landau-Khalatnikov equations of motion (Ginzburg et al., 1980; Landau & Khalatnikov, 1954) of the form

$$m\frac{\partial^2\mathbf{P}}{\partial t^2}+\gamma\frac{\partial\mathbf{P}}{\partial t}=-\boldsymbol{\nabla}_\delta F_E=-\left(D\frac{\partial^2\mathbf{P}}{\partial z^2}-A\mathbf{P}-B\mathbf{P}^3-C\mathbf{P}^5\right)+\mathbf{E}, \tag{33}$$

are used. Here m is a damping parameter and γ a mass parameter;

$$\boldsymbol{\nabla}_\delta=\hat{\mathbf{x}}\frac{\delta}{\delta P_x}+\hat{\mathbf{y}}\frac{\delta}{\delta P_y}+\hat{\mathbf{z}}\frac{\delta}{\delta P_z}, \tag{34}$$

which involves variational derivatives, and we introduce the term variational gradient-operator for it, noting that $\hat{\mathbf{x}}$, $\hat{\mathbf{y}}$ and $\hat{\mathbf{z}}$ are unit vectors in the positive directions of x, y and z, respectively. These equations of motion are analogous to those for a damped mass-spring system undergoing forced vibrations. However here it is the electric field $\mathbf{E}$ that provides the driving impetus for $\mathbf{P}$ rather than a force explicitly. Also, the potential term $\boldsymbol{\nabla}_\delta F_E|_{\mathbf{E}=0}$ is analogous to a nonlinear force-field (through the terms nonlinear in P) rather than the linear Hook's law force commonly employed to model a spring-mass system. The variational derivatives are given by

$$\frac{\delta F}{\delta P_x}=\left(A+3BP_0^2\right)Q_x+B\left(2P_0Q_x^2+P_0Q^2+Q^2Q_x\right)-D\frac{\partial^2Q_x}{\partial z^2}-E_x \tag{35}$$

and

$$\frac{\delta F}{\delta P_\alpha}=\left(A+BP_0^2\right)Q_\alpha+B\left(2P_0Q_xQ_\alpha+Q^2Q_\alpha\right)-D\frac{\partial^2Q_\alpha}{\partial z^2}-E_\alpha,\quad \alpha=y\text{ or }z, \tag{36}$$

where $Q^2=Q_x^2+Q_y^2+Q_z^2$, and $\mathbf{P}$ has been written as a sum of static and dynamic parts,

$$\begin{aligned}P_x(z,t)&=P_0(z)+Q_x(z,t),\\ P_y(z,t)&=0+Q_y(z,t)=Q_y(z,t),\\ P_z(z,t)&=0+Q_z(z,t)=Q_z(z,t).\end{aligned} \tag{37}$$

In doing this we have assumed in-plane polarization $\mathbf{P}_0(z)=(P_0(z),0,0)$ aligned along the x axis. This is done to simplify the problem so that we can focus on the essential features of the response of the ferroelectric film to an incident field. It should be noted that if $\mathbf{P}_0(z)$ had a z component, depolarization effects would need to be taken in to account in the free energy; a theory for doing this has been presented by Tilley (1993). The in-plane orientation avoids this complication. The Landau Khalatnikov equations in Equation (33) are appropriate

for displacive ferroelectrics that are typically used to fabricate thin films (Lines & Glass, 1977; Scott, 1998) with $BaTiO_4$ being a common example.
The equations of motion describe the dynamic response of the polarization to the applied field. Also the polarization and electric field must satisfy the inhomogeneous wave equation derived from Maxwell's equations. The wave equation is given by

$$\frac{\partial^2 E_\alpha}{\partial x^2} - \frac{\epsilon_\infty}{c^2}\frac{\partial^2 E_\alpha}{\partial t^2} = \frac{1}{c^2\epsilon_0}\frac{\partial Q_\alpha}{\partial t^2}, \quad \alpha = x, y, \text{ or } z. \tag{38}$$

where, c is the speed of light in vacuum, ϵ_0 is the permittivity of free space, and ϵ_∞ is the contribution of high frequency resonances to the dielectric response. The reason for including it is as follows. Displacive ferroelectrics, in which it is the lattice vibrations that respond to the electric field, are resonant in the far infrared and terahertz wave regions of the electromagnetic spectrum and that is where the dielectric response calculated from the theory here will have resonances. There are higher frequency resonances that are far from this and involve the response of the electrons to the electric field. Since these resonances are far from the ferroelectric ones of interest here they can be accounted for by the constant ϵ_∞ (Mills, 1998).
Solving Equations (35) to (38) for a given driving field $\mathbf{E}$ will give the relationship between $\mathbf{P}$ and $\mathbf{E}$, and the way that the resulting electromagnetic waves propagate above, below, and in the film can be found explicitly. However to solve the equations it is necessary to postulate a constitutive relationship between $\mathbf{P}$ and $\mathbf{E}$, as this is not given by any of Maxwell's equations (Jackson, 1998). Therefore next we consider the constitutive relation

4. Constitutive relations between P and E

4.1 Time-domain: Response functions

In the perturbation-expansion approach (Butcher & Cotter, 1990) that will be used here the constitutive relation takes the form

$$\mathbf{Q} = \mathbf{P} - \mathbf{P}_0 = \mathbf{Q}^{(1)}(t) + \mathbf{Q}^{(2)}(t) + \ldots + \mathbf{Q}^{(n)}(t) + \ldots, \tag{39}$$

where $\mathbf{Q}^{(1)}(t)$ is linear with respect to the input field, $\mathbf{Q}^{(2)}(t)$ is quadratic, and so on for higher order terms. The way in which the electric field enters is through time integrals and response function tensors as follows (Butcher & Cotter, 1990):

$$\mathbf{Q}^{(1)}(t) = \epsilon_0 \int_{-\infty}^{+\infty} d\tau\, \mathbf{R}^{(1)}(\tau) \cdot \mathbf{E}(t-\tau) \tag{40}$$

$$\mathbf{Q}^{(2)}(t) = \epsilon_0 \int_{-\infty}^{+\infty} d\tau_1 \int_{-\infty}^{+\infty} d\tau_2\, \mathbf{R}^{(2)}(\tau_1, \tau_2) : \mathbf{E}(t-\tau_1)\mathbf{E}(t-\tau_2), \tag{41}$$

and the general term, denoting an nth-order tensor contraction by $\overset{(n)}{|}$, is

$$\mathbf{Q}^{(n)}(t) = \epsilon_0 \int_{-\infty}^{+\infty} d\tau_1 \cdots \int_{-\infty}^{+\infty} d\tau_n\, \mathbf{R}^{(n)}(\tau_1, \ldots, \tau_n) \overset{(n)}{|} \mathbf{E}(t-\tau_1) \cdots \mathbf{E}(t-\tau_n), \tag{42}$$

which in component form, using the summation convention, is given by

$$Q_{\alpha}^{(n)}(t) = \epsilon_0 \int_{-\infty}^{+\infty} d\tau_1 \cdots \int_{-\infty}^{+\infty} d\tau_n \, R_{\alpha\mu_1\cdots\mu_n}^{(n)}(\tau_1,\ldots,\tau_n) E_{\mu_1}(t-\tau_1)\cdots E_{\mu_n}(t-\tau_n), \tag{43}$$

where α and μ take the values x, y and z. The response function $\mathbf{R}^{(n)}(\tau_1,\ldots,\tau_n)$ is real and an nth-order tensor of rank $n+1$. It vanishes when any one of the τ_i time variables is negative, and is invariant under any of the $n!$ permutations of the n pairs $(\mu_1,\tau_1),(\mu_2,\tau_2),\ldots,(\mu_n,\tau_n)$. Time integrals appear because in general the response is not instantaneous; at any given time it also depends on the field at earlier times: there is temporal dispersion. Analogous to this there is spatial dispersion which would require integrals over space. However this is often negligible and is not a strong influence on the thin film calculations that we are considering. For an in-depth discussion see Mills (1998) and Butcher & Cotter (1990).

4.2 Frequency-domain: Susceptibility tensors

Sometimes the frequency domain is more convenient to work in. However with complex quantities appearing, it is perhaps a more abstract representation than the time domain. Also, in the literature it is common that physically many problems start out being discussed in the time domain and the frequency domain is introduced without really showing the relationship between the two. The choice of which is appropriate though, depends on the circumstances (Butcher & Cotter, 1990); for example if the incident field is monochromatic or can conveniently be described by a superposition of such fields the frequency domain is appropriate, whereas for very short pulses of the order of femtoseconds it is better to use the time domain approach.

The type of analysis of ferroelectric films being proposed here is suited to a monochromatic wave or a superposition of them and so the frequency domain and how it is derived from the time domain will be discussed in this section. Instead of the tensor response functions we deal with susceptibility tensors that arise when the electric field $\mathbf{E}(t)$ is expressed in terms of its Fourier transform $\mathbf{E}(\omega)$ via

$$\mathbf{E}(t) = \int_{-\infty}^{+\infty} d\omega \, \mathbf{E}(\omega) \exp(-i\omega t), \tag{44}$$

(45)

where

$$\mathbf{E}(\omega) = \frac{1}{2\pi} \int_{-\infty}^{+\infty} d\tau \, \mathbf{E}(\tau) \exp(i\omega\tau). \tag{46}$$

Equation (44) can be applied to the time domain forms above. The nth-order term in Equation (42) then becomes,

$$\mathbf{Q}^{(n)}(t) = \epsilon_0 \int_{-\infty}^{+\infty} d\omega_1 \cdots \int_{-\infty}^{+\infty} d\omega_n \, \boldsymbol{\chi}^{(n)}(-\omega_\sigma;\omega_1,\ldots,\omega_n) \,\vdots^{(n)}\, \mathbf{E}(\omega_1)\cdots\mathbf{E}(\omega_n) \exp(-i\omega_\sigma t), \tag{47}$$

where

$$\boldsymbol{\chi}^{(n)}(-\omega_\sigma;\omega_1,\ldots,\omega_n)=\int_{-\infty}^{+\infty}d\tau_1\cdots\int_{-\infty}^{+\infty}d\tau_n\,\mathbf{R}^{(n)}(\tau_1,\ldots,\tau_n)\exp\left[i\sum_{j=1}^{n}\omega_j\tau_j\right], \tag{48}$$

which is called the nth-order susceptibility tensor, and, following the notation of Butcher & Cotter (1990),

$$\omega_\sigma=\omega_1+\omega_2+\cdots+\omega_n. \tag{49}$$

As explained by Butcher & Cotter (1990) intrinsic permutation symmetry implies that the components of the susceptibility tensor are such that $\chi^{(n)}_{\alpha\mu_1\cdots\mu_n}(-\omega_\sigma;\omega_1,\ldots,\omega_n)$ is invariant under the $n!$ permutations of the n pairs $(\mu_1,\omega_1),(\mu_2,\omega_2),\ldots,(\mu_n,\omega_n)$.
The susceptibility tensors are useful when dealing with a superposition of monochromatic waves. The Fourier transform of the field then involves delta functions, and the evaluation of the integrals in Equation (47) is straightforward with the polarization determined by the values of the susceptibility tensors at the frequencies involved. Hence, by expanding $\mathbf{Q}(t)$ in the frequency domain,

$$\mathbf{Q}^{(n)}(t)=\int_{-\infty}^{+\infty}d\omega\,\mathbf{Q}^{(n)}(\omega)\exp(-i\omega t), \tag{50}$$

where

$$\mathbf{Q}^{(n)}(\omega)=\frac{1}{2\pi}\int_{-\infty}^{+\infty}d\tau\,\mathbf{Q}^{(n)}(\tau)\exp(i\omega\tau), \tag{51}$$

one may obtain, from Equation (47),

$$\mathbf{Q}^{(n)}(\omega)=\epsilon_0\int_{-\infty}^{+\infty}d\omega_1\cdots\int_{-\infty}^{+\infty}d\omega_n\,\boldsymbol{\chi}^{(n)}(-\omega_\sigma;\omega_1,\ldots,\omega_n)\overset{(n)}{\mid}\mathbf{E}(\omega_1)\cdots\mathbf{E}(\omega_n)\delta(\omega-\omega_\sigma), \tag{52}$$

where we have used the identity (Butcher & Cotter, 1990)

$$\frac{1}{2\pi}\int_{-\infty}^{+\infty}d\omega\,\exp[i\omega(\tau-t)]=\delta(\tau-t), \tag{53}$$

in which δ is the Dirac delta function (not to be confused with an extrapolation length). We have expanded the Fourier component of the polarization $\mathbf{Q}$ at the frequency ω_σ as a power series, so

$$\mathbf{Q}(\omega)=\sum_{r}^{\infty}\mathbf{Q}^{(r)}(\omega). \tag{54}$$

The component form of Equation (52) is

$$\left[Q^{(n)}(\omega)\right]_\alpha=\epsilon_0\int_{-\infty}^{+\infty}d\omega_1\cdots\int_{-\infty}^{+\infty}d\omega_n\,\chi^{(n)}_{\alpha\mu_1\cdots\mu_n}(-\omega;\omega_1,\ldots,\omega_n)\times\left[E(\omega_1)\right]_{\mu_1}\cdots\left[E(\omega_n)\right]_{\mu_n}\delta(\omega-\omega_\sigma). \tag{55}$$

Again the summation convention is used so that repeated Cartesian-coordinate subscripts $\mu_1 \cdots \mu_n$ are to be summed over x, y and z.
Next the evaluation of the integrals in Equation (52) is considered for a superposition of monochromatic waves given by

$$\mathbf{E}(t) = \frac{1}{2} \sum_{\omega' \geqslant 0} \left[\mathbf{E}_{\omega'} \exp(-i\omega' t) + \mathbf{E}_{-\omega'} \exp(i\omega' t) \right] \tag{56}$$

Here, since $\mathbf{E}(t)$ is real, $\mathbf{E}_{-\omega'} = \mathbf{E}^*_{\omega'}$. The Fourier transform of $\mathbf{E}(t)$ from Equation (44) is given by

$$\mathbf{E}(\omega) = \frac{1}{2} \sum_{\omega' \geqslant 0} \left[\mathbf{E}_{\omega'} \delta(\omega - \omega') + \mathbf{E}_{-\omega'} \delta(\omega + \omega') \right]. \tag{57}$$

With $\mathbf{E}(t)$ given by Equation (56), the n-th order polarization term in Equation (47) can be rewritten as

$$\mathbf{Q}^{(n)}(t) = \frac{1}{2} \sum_{\omega' \geqslant 0} \left[\mathbf{Q}^{(n)}_{\omega} \exp(-i\omega t) + \mathbf{Q}^{(n)}_{-\omega} \exp(i\omega t) \right], \tag{58}$$

where $\mathbf{Q}^{(n)}_{-\omega} = \left(\mathbf{Q}^{(n)}_{\omega} \right)^*$ because $\mathbf{Q}^{(n)}(t)$ is real.

By substituting Equation (57) into Equation (52) an expression for $\mathbf{Q}^{(n)}_{\omega}$ can be obtained. The Cartesian μ-component following the notation of Ward (1969) and invoking intrinsic permutation symmetry (Butcher & Cotter, 1990) can be shown to be given by

$$\left(Q^{(n)}_{\omega_\sigma} \right)_{\alpha} = \epsilon_0 \sum_{\omega} K(-\omega_\sigma; \omega_1, \ldots, \omega_n) \chi^{(n)}_{\alpha\mu_1\cdots\mu_n}(-\omega_\sigma; \omega_1, \ldots, \omega_n) (E_{\omega_1})_{\mu_1} \cdots (E_{\omega_n})_{\mu_n}, \tag{59}$$

which in vector notation is

$$\mathbf{Q}^{(n)}_{\omega_\sigma} = \epsilon_0 \sum_{\omega} K(-\omega_\sigma; \omega_1, \ldots, \omega_n) \boldsymbol{\chi}^{(n)}(-\omega_\sigma; \omega_1, \ldots, \omega_n) \stackrel{(n)}{|} \mathbf{E}_{\omega_1} \cdots \mathbf{E}_{\omega_n}. \tag{60}$$

As with Equation (55), the summation convention is implied; the $\sum_\omega$ summation indicates that it is necessary to sum over all distinct sets of $\omega_1, \ldots, \omega_n$. Although in practice, experiments can be designed to avoid this ambiguity in which case there would be only one set and no such summation. K is a numerical factor defined by

$$K(-\omega_\sigma; \omega_1, \ldots, \omega_n) = 2^{l+m-n} p, \tag{61}$$

where p is the number of distinct permutations of $\omega_1, \ldots, \omega_n$, n is the order of nonlinearity, m is the number of frequencies in the set $\omega_1, \ldots, \omega_n$ that are zero (that is, they are d.c. fields) and $l = 1$ if $\omega_\sigma \neq 0$, otherwise $l = 0$.
Equation (59) describes a catalogue of nonlinear phenomena (Butcher & Cotter, 1990; Mills, 1998). For harmonic generation of interest in this chapter, $K = 2^{1-n}$ corresponding to n-th order generation and $-\omega_\sigma; \omega_1, \ldots, \omega_n \rightarrow -n\omega; \omega, \ldots, \omega$. For example second-harmonic generation is described by $K = 1/2$ and $-\omega_\sigma; \omega_1, \ldots, \omega_n \rightarrow -2\omega; \omega, \omega$.

5. Harmonic generation calculations

The general scheme for dealing with harmonic generation based on the application of the theory discussed so far will be outlined and then the essential principles will be demonstrated by looking at a specific example of second harmonic generation.

5.1 General considerations

The constitutive relations discussed in the previous section show how the polarization can be expressed as a power series in terms of the electric field. The tensors appear because of the anisotropy of ferroelectric crystals. However depending on the symmetry group some of the tensor elements may vanish (Murgan et al., 2002; Osman et al., 1998). The tensor components appear as unknowns in the constitutive relations. The Landau-Devonshire theory approach provides a way of calculating the susceptibilities as expressions in terms of the ferroelectric parameters and expressions that arise from the theory. The general problem for a ferroelectric film is to solve the equations of motion in Equation (33) for a given equilibrium polarization profile in the film together with the Maxwell wave equation, Equation (38), by using a perturbation expansion approach where the expansion to be used is given by the constitutive relations and the tensor elements that appear are the unknowns that are found when the equations are solved. Terms that have like electric field components will separate out so that there will be equations for each order of nonlinearity and type of nonlinear process. Starting from the lowest order these equations can be solved one after the other as the order is increased. However for orders higher than three the algebraic complexity in the general case can become rather unwieldy. For nth-order harmonic generation, as pointed out in the previous section, $\omega_\sigma = n\omega$ corresponding to the the terms in Equation (59) given by

$$\left(Q^{(n)}_{n\omega}\right)_\alpha = \epsilon_0 K(-n\omega;\omega,\ldots,\omega)\chi^{(n)}_{\alpha\mu_1\cdots\mu_n}(-n\omega;\omega,\ldots,\omega)(E_\omega)_{\mu_1}\cdots(E_\omega)_{\mu_n}, \tag{62}$$

where the sum over distinct set of frequencies has been omitted but remains implied if it is needed. For calculations involving harmonic generation only the terms in Equation (62) need to be dealt with.

The equations of course can only be solved if the boundary conditions are specified and for the polarization and it is assumed that equations of the form given above in Equation (9) will hold at each boundary. Electromagnetic boundary conditions are also required and these are given by continuity E and H at the boundaries, as demonstrated in the example that follows.

5.2 Second harmonic generation: an example

Here we consider an example of second harmonic generation and choose a simple geometry and polarization profile that allows the essence of harmonic generation calculations in ferroelectric films to be demonstrated whilst at the same time the mathematical complexity is reduced. The solution that results will be applied to finding a reflection coefficient for second harmonic waves generated in the film. This is of practical use because such reflections from ferroelectric films can be measured. Since the main resonances in ferroelectrics are in the far infrared region second harmonic reflections will be in the far infrared or terahertz region. Such reflection measurements will give insight into the film properties, including the size effects that in the Landau-Devonshire theory are modelled by the D term in the free energy expressions and by the extrapolation lengths in the polarization boundary conditions. We will consider a finite thickness film with a free energy given by Equation (17) and polarization

boundary conditions given in Equations (18) and (19), but for the simplest possible case in which the extrapolation lengths approach infinity which implies a constant equilibrium polarization. We consider the ferroelectric film to be on a metal substrate. Assuming that the metal has infinite electrical conductivity then allows a simple electromagnetic boundary conditions to be employed consistent with $\mathbf{E} = 0$ at the ferroelectric-metal interface. The presence of the metal substrate has the advantage that the reflected waves of interest in reflection measurements are greater that for a free standing film since there is no wave transmitted to the metal substrate and more of the electromagnetic energy is reflected at the metal interface compared to a free standing film that transmits some of the energy. The film thickness chosen for the calculations is 40 nm in order to represent the behaviour of nanoscale films.

Note that the focus is on calculating a reflection coefficient for the second harmonic waves reflected from the film. The tensor components do not appear explicitly as we are dealing with ratios of the wave amplitudes for the electric field. However the equations solved provide expressions for the electric field and polarization and from the expressions for the polarization the tensor components can be extracted if desired by comparison with the constitutive relations. There are only a few tensor components in this example because of the simplified geometry and symmetry chosen, as will be evident in the next section.

5.2.1 Some simplifications and an overview of the problem

The incident field is taken to be a plane wave of frequency ω with a wave number above the film of magnitude $q_0 = \omega/c$, since the region above the film behaves like a vacuum in which all frequencies propagate at c. We only consider normal incidence and note that the field is traveling in the negative z direction in the coordinate system used here in which the top of the film is in the plane $z = 0$, the bottom in the plane $z = -L$. Therefore $\mathbf{q}_0 = q_0(-\hat{\mathbf{z}})$ and the incident field can be represented by

$$\frac{1}{2}\left[\mathbf{E}_0 e^{iq_0(-\hat{\mathbf{z}})\cdot z\hat{\mathbf{z}}} e^{-i\omega t} + \mathbf{E}_0^* e^{iq_0(\hat{\mathbf{z}})\cdot z\hat{\mathbf{z}}} e^{i\omega t}\right] = \frac{1}{2}\left[\mathbf{E}_0 e^{-iq_0 z} e^{-i\omega t} + \mathbf{E}_0^* e^{iq_0 z} e^{i\omega t}\right], \tag{63}$$

where

$$\mathbf{E}_0 = E_0[(E_{0x}/|E_0|)\hat{\mathbf{x}} + (E_{0y}/|E_0|)\hat{\mathbf{y}}], \tag{64}$$

written in this way because in general E_0 is a complex amplitude. However, we will take it to be real, so that other phases are measured relative to the incident wave, which, physically, is no loss of generality.

Two further simplifications that will be used are: (i) The spontaneous polarization P_0 will be assumed to be constant throughout the film, corresponding to the limit as δ_1 and δ_2 approach infinity in the boundary conditions of Equations (18) and (19). The equilibrium polarization of the film is then the same as for the bulk described in Section 2.1, and considering a single direction for the polarization, we take

$$P_0(z) = P_0 = \begin{cases} P_B & \text{if } T < T_C, \\ 0 & \text{if } T > T_C, \end{cases} \tag{65}$$

where P_B is given by Equation (5) and $T_C = T_{C0}$. The coupled equations, Equations (35), (36) and (38), can then be solved analytically. Insights into the overall behavior can still be achieved, despite this simplification, and the more general case when $P_0 = P_0(z)$, which

implies a numerical solution, will be dealt with in future work. (ii) Only an x polarized incident field will be considered ($E_{0y} = 0$ in Equation (64)) and the symmetry of the film's crystal structure will be assumed to be uniaxial with the axis aligned with $\mathbf{P}_0 = P_0\hat{\mathbf{x}}$. Under these circumstances $E_\alpha = Q_\alpha = 0, \alpha = y,\ z$, meaning that the equations that need to be solved are reduced to Equations (35), and (38) for $\alpha = z$.

The problem can now be solved analytically. From Equations (39) to (41) it can be seen that, for the single frequency applied field, there will be linear terms corresponding to frequency w and, through $\mathbf{Q}^{(2)}$ in Equation (41), there will be nonlinear terms coming from products of the field components (only those involving E_x^2 for the case we are considering), each involving a frequency 2ω—these are the second harmonic generation terms. It is natural to split the problem in to two parts now: one for the linear terms at ω, the other for the second harmonic generation terms at 2ω. Since we are primarily interested in second harmonic generation it may seem that the linear terms do not need to be considered. However, the way that the second harmonics are generated is through the nonlinear response of the polarization to the linear applied field terms. This is expressed by the constitutive relation in Equation (39), from which it is clear that products of the linear terms express the second harmonic generation, which implies that the linear problem must be solved before the second harmonic generation terms can be calculated. This will be much more apparent in the equations below. In view of this we will deal with the problem in two parts one for the linear terms, the other for the second harmonic generation terms. Also, since we have a harmonic incident field (Equation (63)) the problem will be solved in the frequency domain.

5.2.2 Frequency domain form of the problem for the inear terms

For the linear terms at frequency ω, we seek the solution to the coupled differential equations, Equations (35) and (38) with constitutive relations given by Equations (40) and (41), and a P_0 given by Equation (69). This is expressed in the frequency domain through Fourier transform given in Equations (65) and (66).

The resulting coupled differential equations are

$$D\frac{d^2Q^\omega}{dz^2} + M(\omega)Q^\omega + E^\omega = 0, \tag{66}$$

$$\frac{d^2E^\omega}{dz^2} + \frac{\omega^2\epsilon_\infty}{c^2}E^\omega + \frac{\omega^2}{\epsilon_0 c^2}Q^\omega = 0, \tag{67}$$

for $-L \leqslant z \leqslant 0$, where,

$$M(\omega) = m\omega^2 + i\omega\gamma - 2BP_0^2. \tag{68}$$

Taking the ansatz e^{iqz} for the form of the $Q^\omega$and E^ωsolutions, non trivial solutions (which are the physically meaningful ones) are obtained providing that the determinant of the coefficient matrix—generated by substituting the ansatz into Equations (66) and (67)—satisfies

$$\begin{vmatrix} 1 & -Dq^2 + M(\omega) \\ -q^2 + \frac{\omega^2\epsilon_\infty}{c^2} & \frac{\omega^2}{\epsilon_0 c^2} \end{vmatrix} = 0. \tag{69}$$

This leads to a quadratic equation in q^2 whose solution is

$$(q_j^\omega)^2 = \frac{g_1(\omega)(-1)^{j+1}\sqrt{g_2(\omega)}}{2D}, \quad j = 1, 2, \tag{70}$$

where

$$g_1(\omega) = \frac{D\omega^2\epsilon_\infty}{c^2} + M(\omega), \tag{71}$$

$$g_2(\omega) = g_1^2(\omega) - \frac{4D\omega^2}{\epsilon_0 c^2}\left[\epsilon_\infty\epsilon_0 M(\omega) - 1\right], \tag{72}$$

and the ω dependence of the q solutions has been made explicit with the superscript. The general solution of the coupled equations, Equations (66) and (67) for the electric field is therefore,

$$E^\omega(z) = a_1 E_0 e^{-iq_1^\omega z} + a_2 E_0 e^{iq_1^\omega z} + a_3 e^{-iq_2^\omega z} + a_4 e^{iq_2^\omega z} \tag{73}$$

$$= E_0 \sum_{j=1}^{4} a_j e^{(-1)^j i q_{n_j}^\omega z}, \tag{74}$$

where $n_j = \lceil j/2 \rceil$. It is convenient to include the incident amplitude E_0 as a factor when expressing the constants as this will cancel when the boundary conditions are applied so that the a_1 to a_4 amplitudes are the wave amplitudes of these four waves in the film relative to the incident amplitude. The first term on the right side of Equation (73) is a transmitted wave traveling through the film towards the metal boundary (in the direction of $-z$ in our coordinate system), the second is the wave reflected from the metal boundary and traveling back towards the top of the film corresponding to the wave vectors $-q_1^\omega$ and q_1^ω, respectively; a similar pattern follows for the $\pm q_2^\omega$ modes of the last two terms. It is interesting to note that the presence of both $\pm q_1^\omega$ and $\pm q_2^\omega$ modes is a direct result of the D term in the free energy that is introduced to account for variations in the polarization. In this sense our calculation, despite using a constant P_0 value, is still incorporating the effects of varying polarization (the full effects, as discussed above, involve numerical calculations which will be done in future work). If there was no D term then only the $\pm q_1^\omega$ modes would be present and the character of the solution would be different.

Above the film, alongside the incident wave there is a reflected wave. Thus we have

$$E_1^\omega(z) = E_0 e^{-iq_0 z} + r E_0 e^{iq_0 z}, \quad z > 0 \tag{75}$$

where r is the linear reflection coefficient (there will also be a wave from second harmonic generation which is considered in the next section).

To complete the solution of the linear problem it remains to calculate the a_j and r amplitudes (five in total) by applying boundary conditions. The boundary conditions are the usual electromagnetic boundary conditions of continuity of the electric and magnetic fields, and here, we will express the continuity of the magnetic field as the continuity of $d\mathbf{E}/dz$; this follows from the electromagnetic induction Maxwell equation, $\boldsymbol{\nabla} \times \mathbf{E} = -\partial\mathbf{B}/\partial t$ (since the film is nonmagnetic $\mathbf{B} = \mu_0\mathbf{H}$ not only above the film but also in the film). The boundary conditions on $\mathbf{P}$ in Equations (18) and (19) will also be used, in the limiting case of infinite

extrapolation lengths. In fact, as discussed by Chandra & Littlewood (2007), an infinite extrapolation length for the metal boundary may well be a value consistent with experimental results on films with metal electrodes attached.
In view of the forgoing the required boundary conditions are:

$$E_{\mathrm{I}}^{\omega}(0) = E^{\omega}(0), \;\; \left.\frac{dE_{\mathrm{I}}^{\omega}}{dz}\right|_{z=0} = \left.\frac{dE^{\omega}}{dz}\right|_{z=0}, \;\; \left.\frac{dQ^{\omega}}{dz}\right|_{z=0} = 0, \tag{76}$$

for the top surface, and

$$E^{\omega}(-L) = 0, \;\; \left.\frac{dQ^{\omega}}{dz}\right|_{z=-L} = 0, \tag{77}$$

for the film-metal interface at the bottom. Note that the electric field boundary condition at the bottom implies that the metal conductivity is infinite so that no electric field penetrates the metal. This is a common approximation for metal boundaries and should be sufficient for our purposes since the conductivity of the ferroelectric film is much smaller than for the metal (Webb, 2006). Also the continuity of the magnetic field is not used at the bottom; it is not required because, with five unknowns, five boundary conditions are sufficient to find them.
Applying the boundary conditions leads to a set of simultaneous equations, the solution of which yields expressions for r and the a_j in terms of the other parameters, and hence solves the linear problem. These equations may be expressed in matrix form as

$$\mathsf{M}(\omega)\mathsf{a}_{\mathrm{lin}} = \mathsf{b}_{\mathrm{lin}}, \tag{78}$$

where

$$\mathsf{M}(\omega) = \begin{pmatrix} 1 & 1 & 1 & 1 & -1 \\ q_1^{\omega} & -q_1^{\omega} & q_2^{\omega} & -q_2^{\omega} & q_0 \\ \kappa_1^{\omega} & \kappa_2^{\omega} & \kappa_3^{\omega} & \kappa_4^{\omega} & 0 \\ \Delta_1^{\omega} & \Delta_2^{\omega} & \Delta_3^{\omega} & \Delta_4^{\omega} & 0 \\ \kappa_1^{\omega}\Delta_1^{\omega} & \kappa_2^{\omega}\Delta_2^{\omega} & \kappa_3^{\omega}\Delta_3^{\omega} & \kappa_4^{\omega}\Delta_4^{\omega} & 0 \end{pmatrix}, \tag{79}$$

$$\mathsf{a}_{\mathrm{lin}} = \left(a_1, a_2, a_3, a_4, r\right)^{\mathsf{T}}, \tag{80}$$

$$\mathsf{b}_{\mathrm{lin}} = \left(1, q_0, 0, 0, r\right)^{\mathsf{T}}, \tag{81}$$

and we define

$$\kappa_j^{\omega} = (-1)^j q_{n_j}^{\omega}\left[(q_{n_j}^{\omega})^2 - \epsilon_{\infty} q_0^2\right], \quad \Delta_j^{\omega} = e^{(-1)^{j+1} i q_{n_j} L}. \tag{82}$$

The resulting symbolic solution is rather complicated and will not be given here explicitly. It is easily obtained, however, with a computer algebra program such as Maxima or Mathematica. A more efficient approach for numerical plots is to compute numerical values of all known quantities before solving the matrix equation, which is then reduced to a problem involving the five unknowns multiplied by numerical constants.

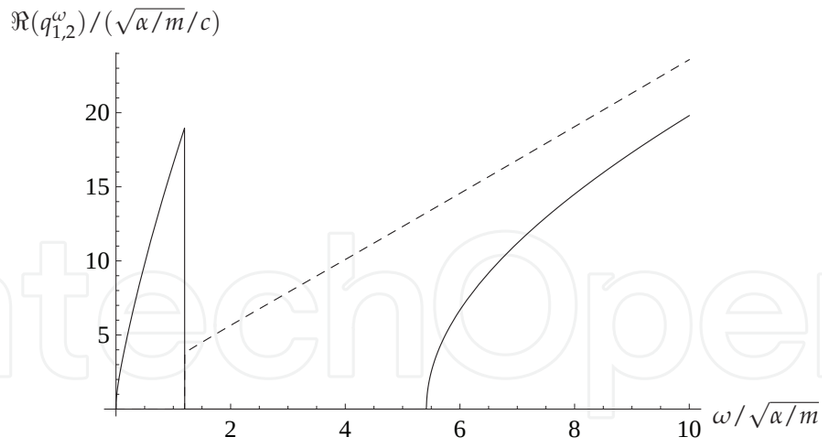

Fig. 4. Dimensionless plot of $\Re(q_1^{\omega})$ and $\Re(q_2^{\omega})$ (dotted line) versus frequency for $a = 6.8 \times 10^5\,\mathrm{V\,K^{-1}A^{-1}s^{-1}}$, $D = 2.7 \times 10^{-21}\,\mathrm{A\,Kg^{-1}m^{-1}}$, $m = 6.4 \times 10^{-21}\,\mathrm{kg\,m^3A^{-1}s^{-2}}$, $L = 40\,\mathrm{nm}$, $T/T_c = 0.5$, $\gamma = 1.3 \times 10^{-9}\,\mathrm{A^{-1}V^{-1}m^{-3}}$, and $\epsilon_\infty = 3.0$. These values are for $BaTiO_4$, and follow Chew et al. (2001).

The real parts of the dispersion relations in Equation (70) are plotted in Figure 4 for the q_1^{ω} and q_2^{ω} modes. The q_1^{ω} mode is the usual mode found in dielectrics and the frequency region, known as the reststrahl region, in which it is zero is where there are no propagating waves for that mode. However, it is clear from the plot that the real part of the q_2^{ω} mode is not zero in this region and so there will be propagation leading to a different reflection coefficient than what would be observed otherwise. This is due to the effect of the D term.
In Figure 5 the magnitude of the reflection coefficient r—available from the solution to the linear problem—is plotted against frequency. With no D term the reflection coefficient would take the value 1 in the reststrahl region. It is clear from the plot that there is structure in this region that is caused by the q_2^{ω} mode. So reflection measurements are a way of investigating the varying polarization modeled through the D term. The plot is for a film thickness of 40 nm. So our model predicts that these effects will be significant for nanoscale films. It is also expected that structure in this region will be found for the second harmonic generation reflection, the calculation of which which we now turn to.

5.2.3 Frequency domain form of the problem for the nonlinear second harmonic generation terms

The second harmonic generation terms come from the second order nonlinear terms, at frequency 2ω and the coupled differential equations that need to be solved for these terms are

$$D\frac{d^2Q^{2\omega}}{dz^2} + M(2\omega)Q^{2\omega} + E^{2\omega} = 3BP_0^2[Q^{\omega}]^2, \tag{83}$$

$$\frac{d^2E^{2\omega}}{dz^2} + \frac{(2\omega)^2\epsilon_\infty}{c^2}E^{2\omega} + \frac{(2\omega)^2}{\epsilon_0 c^2}Q^{2\omega} = 0, \tag{84}$$

$$\text{for } -L \leqslant z \leqslant 0.$$

It can be seen from this that there will be a homogeneous solution analogous to the linear solution but now at frequency 2ω and in addition, due to the term involving $[Q^{\omega}]^2$ in

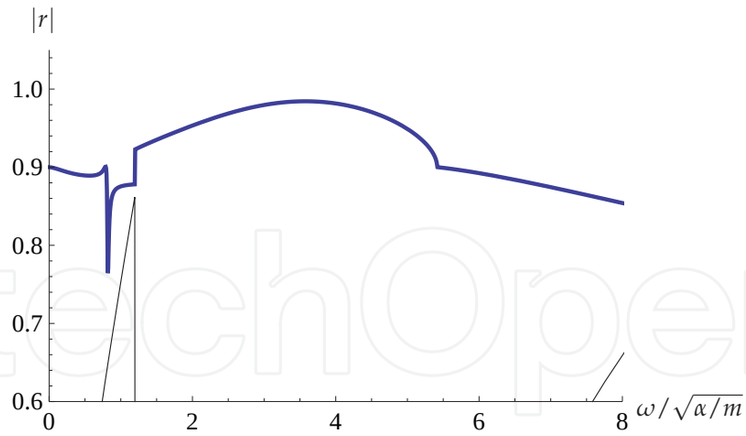

Fig. 5. Magnitude of linear reflection coefficient r versus dimensionless frequency. The lower curve is a scaled down plot of the dispersion curve for q_1^ω showing the reststrahl region. Parameter values as in Figure 4.

Equation (83), there will be particular solutions. $[Q^\omega]^2$ can be found from the solution to the linear problem for E^ω substituted into Equation (67), and thus the particular solutions to Equations (83) and (84) can be determined. In this way the general solution can be shown to be given by

$$E_0^2\Lambda\sum_{j=1}^{4}\phi_j e^{(-1)^j i q_{n_j}^{2\omega} z} + E_0^2\sum_{j=1}^{4}\sum_{k=1}^{4} W_{jk} e^{iB_{jk}z}, \tag{85}$$

together with,

$$W_{jk} = \frac{12BP_0^2 A_{jk}}{\epsilon_0\left[4q_0^2\epsilon_\infty - B_{jk}^2\right]\left[DB_{jk}^2 - M(2\omega)\right]}, \tag{86}$$

$$A_{jk} = S_{n_j}S_{n_k}a_j a_k, \tag{87}$$

$$s_j = (q_j^\omega)^2 - \epsilon_\infty\omega/c^2, \tag{88}$$

$$B_{jk} = (-1)^j q_{n_j}^\omega + (-1)^k q_{n_k}^\omega. \tag{89}$$

It is convenient to include the factor E_0^2 in Equation (85) since it will cancel out later when the boundary conditions are applied. The factor Λ has been included to make the ϕ_j amplitudes dimensionless so that they are on the same footing as the a_j amplitudes in the linear problem. Due to the second harmonic generation terms in the film there will also be a second harmonic generation field transmitted from the film to the air above, but since this ultimately exists because of the incident field the second harmonic generation wave above the film is a reflected wave caused by the incident field. It is expressed by

$$E_{\mathrm{I}}^{2\omega}(z) = E_0^2\Lambda\rho e^{2iq_0 z}, \quad z > 0, \tag{90}$$

where ρ is the second harmonic generation reflection coefficient.
Again there are five unknowns: ρ and the ϕ_j, which are also found by applying the boundary conditions. The particular solutions make the problem more complex algebraically, but in principle the solution method is the same as for the linear case. Applying the conditions in

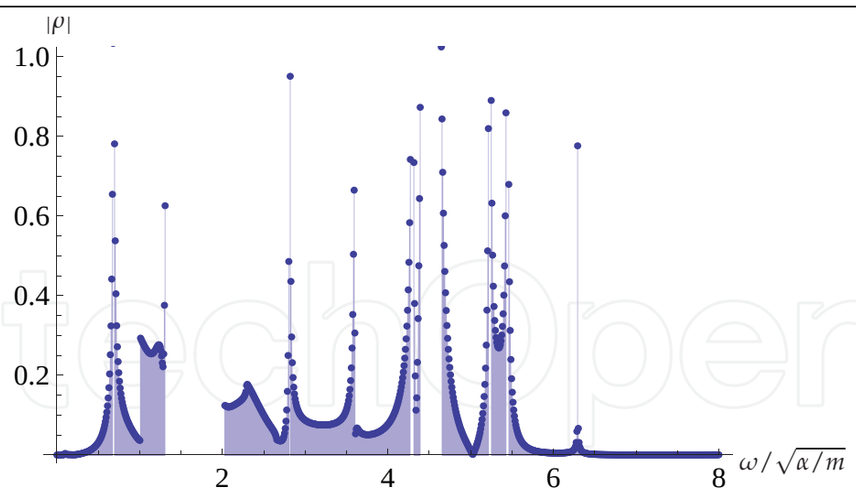

Fig. 6. Second harmonic generation reflection coefficient ρ versus dimensionless frequency. Parameter values are as in Figure 4.

Equations (76) and (77) leads to five simultaneous equations that can be expressed as

$$\mathsf{M}(2\omega)\mathsf{a}_{\mathrm{SHG}} = \mathsf{b}_{\mathrm{SHG}}, \tag{91}$$

where

$$\mathsf{a}_{\mathrm{SHG}} = \left(\phi_1, \phi_2, \phi_3, \phi_4, \rho\right)^{\mathsf{T}}, \tag{92}$$

$$\mathsf{b}_{\mathrm{SHG}} = \left(\mathcal{P}_1, \mathcal{P}_2, \mathcal{P}_3, \mathcal{P}_4, \mathcal{P}_5\right)^{\mathsf{T}}, \tag{93}$$

with

$$\left.\begin{aligned} \mathcal{P}_1 = -(1/\Lambda)\sum_{jk} W_{jk},\ \mathcal{P}_2 = (1/\Lambda)\sum_{jk} W_{jk}B_{jk}, \\ \mathcal{P}_3 = (1/\Lambda)\sum_{jk} W_{jk}O_{jk},\ \mathcal{P}_4 = -(1/\Lambda)\sum_{jk} W_{jk}\delta_{jk}, \\ \mathcal{P}_5 = (1/\Lambda)\sum_{jk} W_{jk}O_{jk}\delta_{jk}, \end{aligned}\right\} \tag{94}$$

and

$$O_{jk} = B_{jk}\left(4\epsilon_\infty q_0^2 - B_{jk}^2\right), \quad \delta_{jk} = e^{-iB_{jk}L}. \tag{95}$$

Now the unknowns for the second harmonic generation problem can be found by solving Equation (91), in a similar way to what was done for the linear problem, and from this the second harmonic generation reflection coefficient ρ can be found.
A plot of $|\rho|$ versus frequency is given in Figure 6. A dramatic structure is evident and, as with the linear reflection, is also present in the reststrahl region. So second harmonic generation reflection measurements are expected to be a sensitive probe of size effects in nanoscale ferroelectric thin films according to the model presented here.

The numerical values calculated for the second harmonic generation reflection coefficient are much smaller than for the linear one. This is to be expected since second harmonic generation is a second-order nonlinear effect. This numerical result is consistent with that found by Murgan et al. (2004), but their work did not include the mode due to the D term. Also the general features of the second harmonic generation reflection coefficient are similar to a brief second harmonic generation study that was done by Stamps & Tilley (1999) for a free standing film. However the effect of the metal substrate considered here has made the second harmonic generation reflection features more pronounced.

It is also of interest to compare the numerical values here with experimental studies. Many second harmonic generation reflection experimental studies have covered optical frequencies higher than the far-infrared frequencies that are relevant to the work in this paper. It is hoped that our work will stimulate more experimental work in the far-infrared region. Detailed numerical work that is now in progress can then be compared with such experiments.

6. Conclusion

This chapter has considered how Landau-Devonshire theory together with Landau-Khalatnikov equations of motion can be used to model a ferroelectric film. A fairly general theory encompassing size effect that cause the equilibrium polarization to be influenced by surfaces together with the nonlinear dynamical response to incident electromagnetic waves has been given. Then, a specific example of second harmonic generation in ferroelectric films was presented with an emphasis on calculating the reflection coefficient that is relevant to far infrared reflection measurements. It has been shown how the theory suggests that such reflection measurements would enable the ferroelectric properties of the film such as the size effects to be probed.

Some of the more general aspects of the theory are not really needed for this specific example but an aim of presenting the more general formulae is to provide a foundation for the many other calculations that could be done, both linear and nonlinear. A large number of different nonlinear effects could be studied. Also the incorporation of a space varying equilibrium polarization profile of the sort given in Sections 2.2 and 2.3 into the dynamical calculations would be provide a more detailed study than the example given here. Also it would be of use to find a general set of formula that expresses the set of equations that need to be solved for the reflection problem due to general nth-order second harmonic generation. Currently the set of equations for each order has to be derived for each case since no general formulae of for this seems to exist in the literature. The generalization is not entirely trivial, but some progress along those lines as been made by (Webb, 2003; 2009; Webb & Osman, 2003), but quite a lot more needs to be done to produce the set of equations for the nth-order reflection problem.

7. References

Abramowitz, M. & Stegun, I. A. (eds) (1972). *Handbook of Mathematical Functions*, Dover, New York.

Butcher, P. N. & Cotter, D. (1990). *The Elements of Nonlinear Optics*, Cambridge University Press, Cambridge, UK.

Chandra, P. & Littlewood, P. B. (2007). A landau primer for ferroelectrics, *in* K. Rabe, C. H. Ahn & J. M. Triscone (eds), *Physics of Ferroelectrics*, Vol. 105 of *Topics in Applied Physics*, Springer, Heidelberg, p. 69.

Chew, K. H., Ong, L. H., Osman, J. & Tilley, D. R. (2001). Theory of far-infrared reflection and transmission by ferroelectric thin films, *J. Opt. Soc. Am B* 18: 1512.

Cottam, M. G., Tilley, D. R. & Zeks, B. (1984). Theory of surface modes in ferroelectrics, *J. Phys C* 17: 1793–1823.

Gerbaux, X. & Hadni, A. (1989). Far infrared and phase transitions in ferroelectric materials, *Phase Transitions* 14: 117.

Gerbaux, X. & Hadni, A. (1990). *Static and dynamic properties of ferroelectric thin film memories*, PhD thesis, University of Colorado.

Gerbaux, X., Hadni, A. & Kitade, A. (1989). Far ir spectra of ferroelectric Rochelle Salt and sodium ammonium tartrate, *Phys. Stat. Sol. (a)* 115: 587.

Ginzburg, V. L., Levanyuk, A. P. & Sobyanin, A. A. (1980). Light scattering near phase transition points in solids, *Phys. Rep.* 57: 151.

Höchli, U. T. & Rohrer, H. (1982). Separation of the D_{4h} and O_h phases near the surface of $SrTiO_3$, *Phys. Rev Lett.* 48: 188.

Iniguez, J., Ivantchev, S. & Perez-Mato, J. M. (2001). Landau free energy of $BaTiO_3$ from first principles, *Phys. Rev. B* 63: 144103.

Jackson, J. D. (1998). *Classical Electrodynamics*, 3rd edn, Wiley, New York.

Kulkarni, A., Rohrer, G., Narayan, S. & McMillan, L. (1988). Electrical properties of ferroelectric thin film KNO_3 memory devices, *Thin Solid Films* 164: 339.

Landau, L. D. & Khalatnikov, I. M. (1954). On the anomalous absorption of sound near a second-order phase transition point, *Dok. Akad. Navk SSSR* 96: 469.

Li, S., Eastman, J. A., Li, Z., Foster, C. M., Newnham, R. E. & Cross, L. E. (1996). Size effects in nanostructured ferroelectrics, *Phys. Lett.* 212: 341.

Li, S., Eastman, J. A., Vetrone, J. M., Foster, C. M., Newnham, R. E. & Cross, L. E. (1997). Dimension and size effects in ferroelectrics, *Jap. J. Appl. Phys.* 36: 5169.

Lines, M. E. & Glass, A. M. (1977). *Principles and Applications of Ferroelectrics and Related Materials*, Clarendon, Oxford, UK.

Marquardt, P. & Gleiter, H. (1982). Ferroelectric phase transition in microcrystals, *Phys. Rev. Lett.* 48: 1423.

Mills, D. L. (1998). *Nonlinear Optics*, second edn, Springer, Berlin.

Mishina, E. D., Sherstyuk, N. E., Barsky, D., Sigov, A. S., Golovko, Y. I., Mukhorotov, V. M., Santo, M. D. & Rasing, T. (2003). Domain orientation in ultrathin (Ba,Sr)TiO_3 films measured by optical second harmonic generation, *J. Appl. Phys* 93: 6216.

Murgan, R., Razak, F., Tilley, D. R., Tan, T. Y., Osman, J. & Halif, M. N. A. (2004). Second harmonic generation from a ferroelectric film, *Comp. Mat. Sci* 30: 468.

Murgan, R., Tilley, D. R., Ishibashi, Y., Webb, J. F. & Osman, J. (2002). Calculation of nonlinear susceptibility tensor components in ferroelectrics: Cubic, tetragonal, and rhombohedral symmetries, *J. Opt. Soc. Am. B* 19: 2007.

Osman, J., Ishibashi, Y. & Tilley, D. R. (1998). Calculation of nonlinear susceptibility tensor components in ferroelectrics, *Jpn. J. Appl. Phys* 37: 4887.

Scott, J. F. (1998). The physics of ferroelectric ceramic thin films for memory applications, *Ferroelectr. Rev.* 1: 1.

Scott, J. F. & Araujo, C. (1989). Ferroelectric memories, *Science* 246: 1400.

Stamps, R. L. & Tilley, D. R. (1999). Possible far infrared probes of ferroelectric size effects, *Ferroelectrics* 230: 221.

Strukov, B. A. & Lenanyuk, A. P. (1998). *Ferroelectric Phenomena in Crystals*, Springer, Berlin.

Tan, E. K., Osman, J. & Tilley, D. R. (2000). First-order phase transitions in ferroelectric films, *Solid State Communications* 116: 61–65.

Tilley, D. R. (1993). Phase transitions in thin films, *in* N. Setter & E. L. Colla (eds), *Ferroelectric Ceramics*, Birkhäuser Verlag, Berlin, p. 163.

Tilley, D. R. (1996). Finite-size effects on phase transitions in ferroelectrics, *in* C. P. de Araujo, J. F. Scott & G. W. Taylor (eds), *Ferroelectric Thin Films: Synthesis and Basic Properties*, Integrated Ferroelectric Devices and Technologies, Gordon and Breach, Amsterdam, p. 11.

Tilley, D. R. & Zeks, B. (1984). Landau theory of phase transtions in thick films, *Solid State Commun.* 49: 823.

Ward, J. F. (1969). Optical third harmonic generation in gases by a focused laser beam, *Phys. Rev.* 185: 57.

Webb, J. F. (2003). A general approach to perturbation theoretic analysis in nonlinear optics and its application to ferroelectrics and antiferroelectrics, *Int. J. Mod. Phys. B* 17: 4355.

Webb, J. F. (2006). Theory of size effects in ferroelectric ceramic thin films on metal substrates, *J. Electroceram.* 16: 463.

Webb, J. F. (2009). A definitive algorithm for selecting perturbation expansion terms applicable to the nonlinear dynamics of ferroelectrics and cad-modeling, *Proceedings of the International Conference on Computational Design in Engineering (CODE 2009)*, Seoul, Korea.

Webb, J. F. & Osman, J. (2003). Derivation of nonlinear susceptibility coefficients in antiferroelectrics, *Microelectronic Engineering* 66: 584.

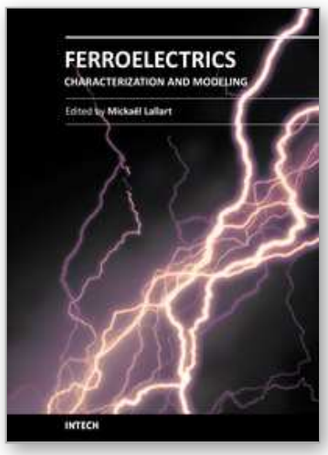

Ferroelectrics - Characterization and Modeling

Edited by Dr. MickaÃ«l Lallart

ISBN 978-953-307-455-9
Hard cover, 586 pages
Publisher InTech
Published online 23, August, 2011
Published in print edition August, 2011

Ferroelectric materials have been and still are widely used in many applications, that have moved from sonar towards breakthrough technologies such as memories or optical devices. This book is a part of a four volume collection (covering material aspects, physical effects, characterization and modeling, and applications) and focuses on the characterization of ferroelectric materials, including structural, electrical and multiphysic aspects, as well as innovative techniques for modeling and predicting the performance of these devices using phenomenological approaches and nonlinear methods. Hence, the aim of this book is to provide an up-to-date review of recent scientific findings and recent advances in the field of ferroelectric system characterization and modeling, allowing a deep understanding of ferroelectricity.

INTECH
open science | open minds

InTech Europe
University Campus STeP Ri
Slavka Krautzeka 83/A
51000 Rijeka, Croatia
Phone: +385 (51) 770 447
Fax: +385 (51) 686 166
www.intechopen.com

InTech China
Unit 405, Office Block, Hotel Equatorial Shanghai
No.65, Yan An Road (West), Shanghai, 200040, China
中国上海市延安西路65号上海国际贵都大饭店办公楼405单元
Phone: +86-21-62489820
Fax: +86-21-62489821

IntechOpen